Hindawi
International Journal of Optics
Volume 2018, Article ID 3153614, 5 pages
https://doi.org/10.1155/2018/3153614

Research Article

Continuous-Wave and Passively Q-Switched Er:Y_2O_3 Ceramic Laser at 2.7 μm

Zhipeng Qin,[1] Guoqiang Xie,[1] Jian Zhang,[2] Jingui Ma,[1] Peng Yuan,[1] and Liejia Qian[1]

[1] *Key Laboratory for Laser Plasmas (Ministry of Education), Collaborative Innovation Center of IFSA (CICIFSA), School of Physics and Astronomy, Shanghai Jiao Tong University, Shanghai 200240, China*
[2] *Key Laboratory of Transparent and Opto-Functional Advanced Inorganic Materials, Shanghai Institute of Ceramics, Chinese Academy of Sciences, Shanghai 201899, China*

Correspondence should be addressed to Guoqiang Xie; xiegq@sjtu.edu.cn

Received 16 August 2017; Revised 9 December 2017; Accepted 28 December 2017; Published 1 March 2018

Academic Editor: Wonho Jhe

We report on a continuous-wave (CW) and passively Q-switched Er:Y_2O_3 ceramic laser in mid-infrared spectral region. In the CW regime, a maximum output power of 2.07 W is achieved at 2717.3 nm with a slope efficiency of 13.5%. Stable passive Q-switching of the Er:Y_2O_3 ceramic laser is demonstrated based on semiconductor saturable absorber mirror. Under an absorbed pump power of 12.4 W, a maximum average output power of 223 mW is generated with a pulse energy of 1.7 μJ and a pulse width of 350 ns at 2709.3 nm.

1. Introduction

Mid-infrared coherent resources in the 2~5 μm spectral range have attracted more and more attention due to the potential applications in spectroscopy, medical treatment, security and defense, free-space communication, and advanced sensing technologies for trace gas detection and greenhouse gas monitoring [1–5]. Rare-earth-doped laser is a general way to generate high-power and high-beam-quality mid-infrared coherent resource [6–8].

Er-doped solid-state lasers can be emitted in the spectral range of 2.7~3.0 μm by electronic transition ($^4I_{11/2} \rightarrow {}^4I_{13/2}$). So far, Er:YAG has been widely used for commercial 2.94 μm laser. For mid-infrared Er:YAG lasers, high Er-doping concentration (50%) is required to overcome self-terminating phenomenon which is caused by a long lifetime of lower laser level [9, 10]. Although high doping concentration can reduce the population in lower laser level by enhancing the energy transfer upconversion process ($^4I_{13/2}+{}^4I_{13/2} \rightarrow {}^4I_{9/2}+{}^4I_{15/2}$), it will bring serious thermal effects due to heat deposited in a small region, which will limit the available output power and beam quality. Er:Y_2O_3 is an excellent alternative for mid-infrared solid-state laser materials. For Er:Y_2O_3 gain medium, a much lower doping concentration (e.g., 2%~7%) is feasible for laser emission [11–14], which significantly alleviates the thermal effects. Besides, Er:Y_2O_3 has a larger product of emission cross section (~1×10^{-19} cm^2) and upper laser level lifetime (2.4 ms) in comparison with Er:YAG [14], which is favorable to achieve a high laser gain. Due to the high melting point, the growth of Er:Y_2O_3 single crystal is challenging. Er:Y_2O_3 ceramic has similar optical performances to the Er:Y_2O_3 single crystal, and the ceramic possesses the advantages of short fabrication period, large size, and low cost. So far, CW operation of Er:Y_2O_3 ceramic laser at room temperature has been reported with an output power of 320 mW and a slope efficiency of 6.5% [12]. At cryogenic temperature of 77 K, a CW output power of 14 W was generated [13]. For passive Q-switching operation, only an average power of 6 mW was generated in Er:Y_2O_3 ceramic laser [11]. Besides, passively Q-switched lasers in Er:CaF_2, Er:SrF_2, Er:Lu_2O_3, and Er:Pr:GGG crystals were also reported (Table 1) [15–19].

Here we demonstrate a passively Q-switched Er:Y_2O_3 ceramic laser at the wavelength of 2.7 μm. In the CW regime, an output power of 2.07 W is obtained with a slope efficiency of 13.5%. The Q-switched operation is realized based on

Table 1: Passively Q-switched Er-doped bulk lasers near 3 μm spectral region.

Gain medium	SA	P_{ave} [mW]	λ_0 [μm]	τ [ns]	E [μJ]	P_{peak} [W]	Ref.
$Er:Y_2O_3$	BP	6	2.72	4470	0.48	0.1	[11]
$Er:CaF_2$	Graphene	172	2.80	1324	2.74	2.1	[15]
$Er:SrF_2$	BP	180	2.79	702	2.34	3.3	[16]
$Er:Lu_2O_3$	MoS_2	1030	2.84	335	8.5	25.4	[17]
$Er:Lu_2O_3$	C_3N_4	1090	2.840	351	11.1	31.6	[18]
Er:Pr:GGG	Graphene	186	2.71	360	1.54	4.3	[19]
$Er:Y_2O_3$	SESAM	223	2.71	350	1.71	4.9	This work

SA, saturable absorber; P_{ave}, average power; P_{peak}, peak power.

SESAM. Under an absorbed pump power of 12.4 W, the Q-switched $Er:Y_2O_3$ ceramic laser emits an average power of 223 mW with a pulse width of 350 ns at repetition rate of 130.6 kHz, resulting in a pulse energy of 1.7 μJ.

2. Experimental Setup

The experimental setup schematics of CW and passively Q-switched $Er:Y_2O_3$ ceramic laser are shown in Figure 1. A commercial 970 nm laser diode (LD) was adopted as the pump source, delivering a maximum power of 30 W from a multimode fiber with a core diameter of 105 μm and a numerical aperture of 0.22. After collimating and focusing by a pair of lenses F_1 and F_2 (f_1 = 18 mm and f_2 = 75 mm), the pump light was imaged into the gain medium. The gain medium of $Er:Y_2O_3$ ceramic had a length of 6.6 mm, a cross section of $2 \times 3\,mm^2$, and an Er-doping concentration of 7%. In order to remove the generated heat while pumping, the $Er:Y_2O_3$ ceramic was wrapped in indium foil and tightly fixed in a copper holder which was cooled by a thermoelectric cooler. The gain medium was antireflectively coated for both pump and laser wavelengths ($R < 0.5\%$). For CW operation, a linear cavity structure was adopted (Figure 1(a)), which consisted of a plane-concave input mirror M_1 (ROC = 50 mm) and a plane-plane output coupler (OC). Figure 1(b) shows the experimental setup schematic of SESAM Q-switched laser.

$Er:Y_2O_3$ ceramic laser had a total cavity length of 25 mm. The employed SESAM (SAM-2400-1-10ps-e, BATOP GmbH) has total absorbance of 5% and 18% at 2700 nm and 2717 nm, respectively.

3. Results and Discussion

3.1. CW Laser Performance. We used different OCs (T = 1%, 3%, and 5%, resp.) to test the CW output powers. Figure 2(a) shows the CW output power versus absorbed pump power with an optimal OC (T = 5%). The laser threshold was ~1.6 W. The output laser power increased linearly with absorbed pump power with a slope efficiency of 13.5%. A maximum CW power of 2.07 W was generated. The output power rollover was not observed even at the maximum pump power, indicating that CW output power could be further increased with higher pump power. At the CW output power of 1 W, we measured the output spectrum, as shown in Figure 2(b). The spectrum peak is at 2717.3 nm with a full width at half maximum (FWHM) of 4.6 nm. With the knife-edge method, we measured the beam quality of CW output laser. The measured M^2 factor of the beam was 2.84 (Figure 2(c)). We also captured the output beam profile with a thermosensitive card (VRC6S, Thorlabs). The inset of Figure 2(c) shows that the laser beam has a round beam profile. In order to test the power stability of the $Er:Y_2O_3$ ceramic laser, we monitored the output power fluctuation for one hour, as shown in Figure 2(d). The output power fluctuation (Δ_{RMS}, the ratio of root-mean-square error to average value) is ~0.65%, indicating that the output power of $Er:Y_2O_3$ ceramic laser is stable.

3.2. SESAM Q-Switched $Er:Y_2O_3$ Laser. In the Q-switched $Er:Y_2O_3$ ceramic laser, we employed a plane-concave OC with transmission of 1%. After introducing the SESAM in the cavity, laser threshold was significantly increased due to the absorption loss of SESAM. The laser threshold was 4.8 W of absorbed pump power. As the absorbed pump power was increased to 9.5 W, Q-switching operation was initiated. Q-switched pulse train was captured by a mid-infrared photodetector (VIGO system, PCI-9) and displayed on a digital oscillator, as shown in Figure 3(a). In order to achieve short Q-switched pulses, we built up a short laser cavity of 25 mm, which emitted the shortest pulse of 350 ns (Figure 3(b)).

Figure 4(a) shows the output power, pulse energy, and peak power evolution with the absorbed pump power. They all increase with the absorbed pump power. At the absorbed pump power of 12.4 W, we obtained a maximum average output power of 223 mW and a maximum pulse energy of 1.7 μJ, corresponding to the peak power of 4.9 W. Beyond the absorbed pump power of 12.4 W, the laser quenching appeared. The laser quenching phenomenon can be attributed to serious thermal lens effect in the gain medium, which results in formation of instable cavity. The focal length of thermal lens was directly measured to be 35 mm at the absorbed pump power of 12.4 W. We added the thermal lens to ABCD propagation matrix and the formation of instable cavity was verified by the numerical calculation. The Q-switched pulse could be recovered by slightly decreasing the incident pump power. The evolution of repetition rate and pulse width with absorbed pump power is shown

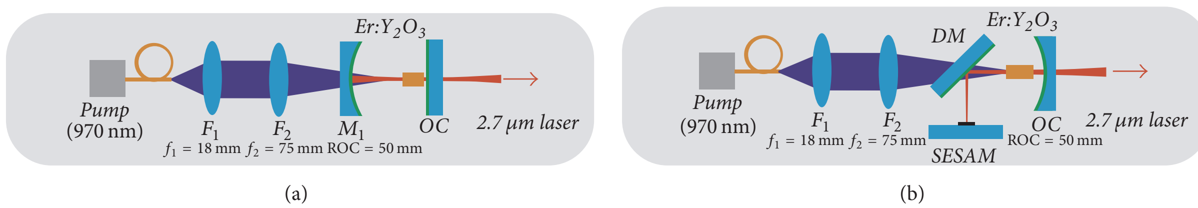

FIGURE 1: Experimental setup schematic of $Er:Y_2O_3$ ceramic laser in CW operation (a) and Q-switching operation (b). ROC: radius of curvature; OC: output coupler; DM: dichroic mirror; SESAM: semiconductor saturable absorber mirror.

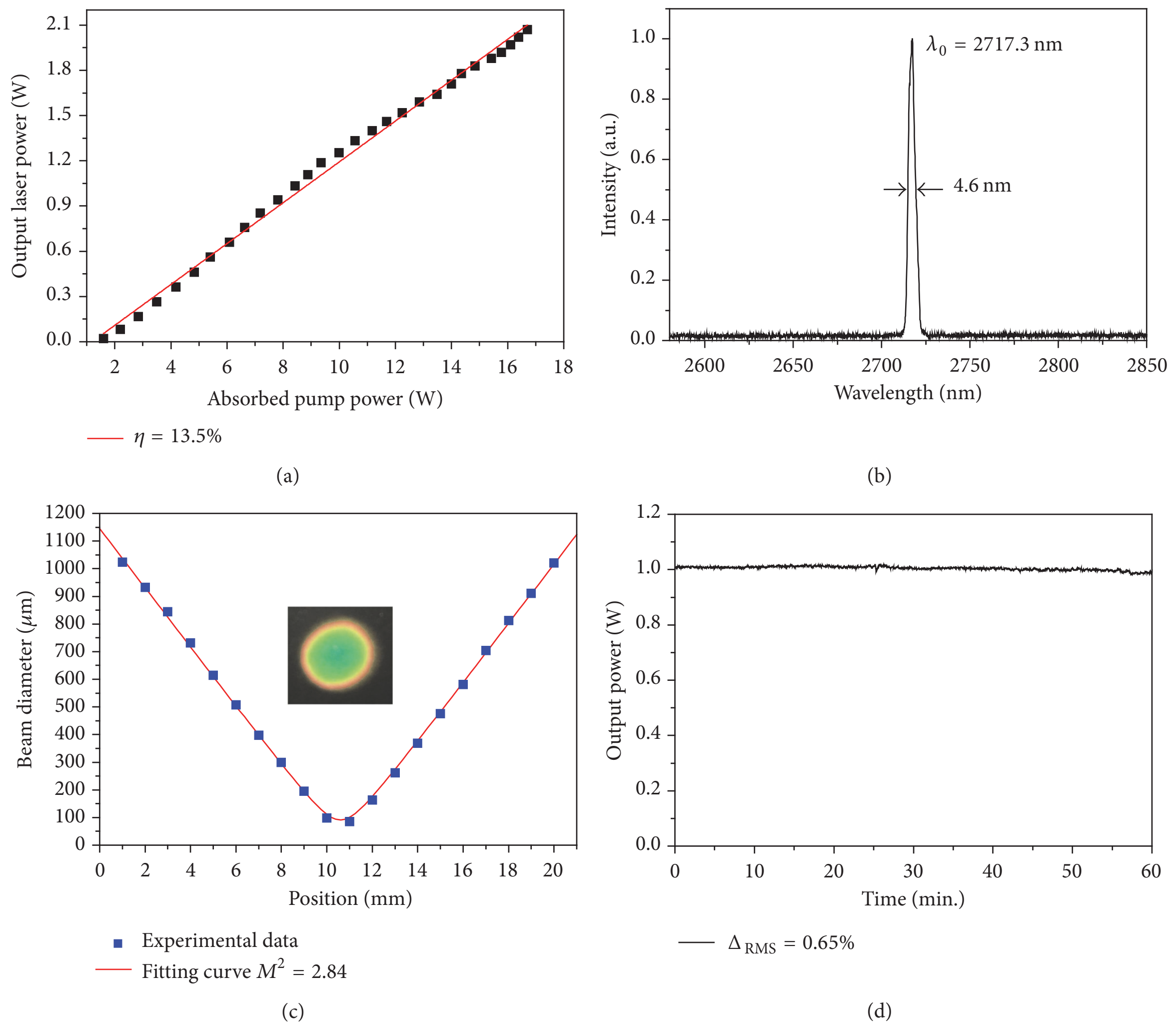

FIGURE 2: (a) CW output power versus absorbed pump power. (b) Spectrum of CW laser. (c) Measurement of the beam quality. Inset: beam profile. (d) CW output power stability of $Er:Y_2O_3$ ceramic laser.

in Figure 4(b). The pulse repetition rate increased from 105.3 kHz to 130.6 kHz in the absorbed pump power range of 9.5~12.4 W. However, the pulse duration decreased from 434 ns to 350 ns and it tended to saturate beyond the absorbed pump power of 12 W.

Figure 5 shows the Q-switched pulse spectrum. The spectral peak is at 2709.3 nm with a FWHM of 2.4 nm. Compared with the CW spectrum, there is a blue shift in Q-switching pulse spectrum, which could be attributed to the larger loss (18%) of the SESAM, measured at the wavelength of 2717 nm. Consequently, the Q-switched $Er:Y_2O_3$ ceramic laser was forced to oscillate at shorter wavelength of 2709 nm. At this wavelength, the Q-switched $Er:Y_2O_3$ ceramic laser suffered from an reabsorption loss under high pump power [12], which dramatically reduced the average output power.

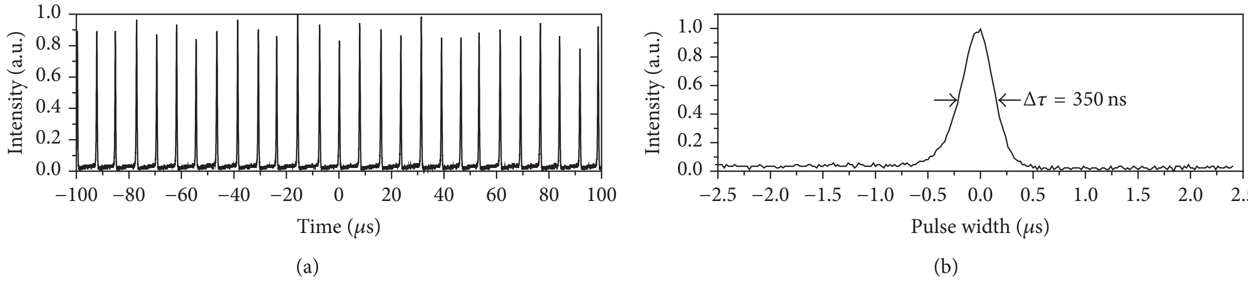

Figure 3: (a) Typical pulse train of passively Q-switched $Er:Y_2O_3$ ceramic laser. (b) Single pulse profile.

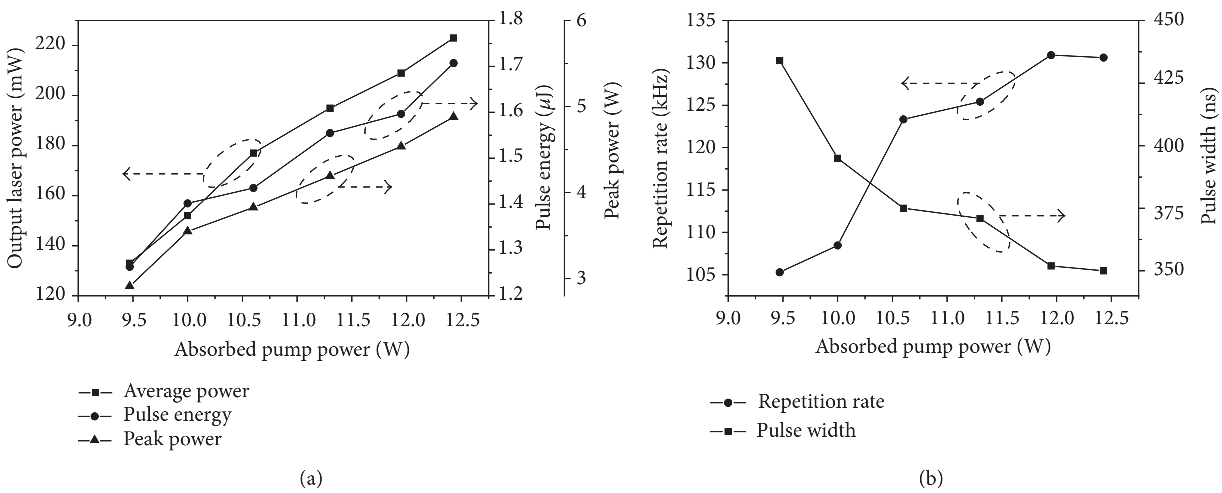

Figure 4: (a) Average output power, pulse energy, and peak power evolution with absorbed pump power. (b) Pulse repetition rate and pulse width evolution with absorbed pump power.

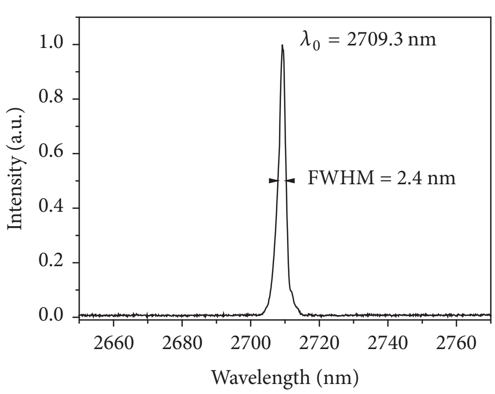

Figure 5: Optical spectrum of the Q-switched pulse.

4. Conclusions

In conclusion, we experimentally demonstrated a CW and passively Q-switched $Er:Y_2O_3$ ceramic laser at 2.7 μm wavelength. A maximum CW output power of 2.07 W was achieved with a slope efficiency of 13.5%. In Q-switching operation, the laser emitted stable Q-switched pulses with an average output power of 223 mW, a pulse energy of 1.7 μJ, a pulse width of 350 ns, and a repetition rate of 130.6 kHz at 2709.3 nm. Our research results show that $Er:Y_2O_3$ ceramic is an excellent gain material for CW and Q-switched laser at 2.7 μm wavelength.

Conflicts of Interest

The authors declare that they have no conflicts of interest.

Acknowledgments

This work is partially supported by the National Basic Research Program of China (Grant no. 2013CBA01505), the Shanghai Excellent Academic Leader Project (Grant no. 15XD1502100), the National Natural Science Foundation of China (Grant no. 61675130), the National Postdoctoral Program for Innovative Talents (no. 190375), and the project funded by China Postdoctoral Science Foundation (no. 190375).

References

[1] B. G. Lee, M. A. Belkin, R. Audet et al., "Widely tunable single-mode quantum cascade laser source for mid-infrared spectroscopy," *Applied Physics Letters*, vol. 91, no. 23, Article ID 231101, 2007.

[2] R. Kaufmann and R. Hibst, "Pulsed 2-94-μm erbium–YAG laser skin ablation—experimental results and first clinical application," *Clinical and Experimental Dermatology*, vol. 15, no. 5, pp. 389–393, 1990.

[3] V. W. S. Chan, "Optical space communications," *IEEE Journal of Selected Topics in Quantum Electronics*, vol. 6, no. 6, pp. 959–975, 2000.

[4] D. Halmer, S. Thelen, P. Hering, and M. Mürtz, "Online monitoring of ethane traces in exhaled breath with a difference frequency generation spectrometer," *Applied Physics B: Lasers and Optics*, vol. 85, no. 2-3, pp. 437–443, 2006.

[5] J. J. Scherer, J. B. Paul, H. J. Jost, and M. L. Fischer, "Mid-IR difference frequency laser-based sensors for ambient CH4, CO, and N2O monitoring," *Applied Physics B: Lasers and Optics*, vol. 110, no. 2, pp. 271–277, 2013.

[6] Z. Qin, G. Xie, C. Zhao, S. Wen, P. Yuan, and L. Qian, "Mid-infrared mode-locked pulse generation with multilayer black phosphorus as saturable absorber," *Optics Expresss*, vol. 41, no. 1, pp. 56–59, 2016.

[7] Z. Qin, G. Xie, H. Zhang et al., "Black phosphorus as saturable absorber for the Q-switched Er:ZBLAN fiber laser at 2.8 μm," *Optics Express*, vol. 23, no. 19, pp. 24713–24718, 2015.

[8] S. B. Mirov, V. V. Fedorov, D. Martyshkin, I. S. Moskalev, M. Mirov, and S. Vasilyev, "Progress in Mid-IR Lasers Based on Cr and Fe-Doped II-VI Chalcogenides," *IEEE Journal of Selected Topics in Quantum Electronics*, vol. 21, no. 1, 2015.

[9] E. Arbabzadah, S. Chard, H. Amrania, C. Phillips, and M. Damzen, "Comparison of a diode pumped Er:YSGG and Er:YAG laser in the bounce geometry at the 3 μm transition," *Optics Express*, vol. 19, no. 27, pp. 25860–25865, 2011.

[10] C. Ziolek, H. Ernst, G. F. Will, H. Lubatschowski, H. Welling, and W. Ertmer, "High-repetition-rate, high-average-power, diode-pumped 2.94-μm Er:YAG laser," *Optics Expresss*, vol. 26, no. 9, pp. 599–601, 2001.

[11] L. Kong, Z. Qin, G. Xie et al., "Black phosphorus as broadband saturable absorber for pulsed lasers from 1 μm to 2.7 μm wavelength," *Laser Physics Letters*, vol. 13, no. 4, Article ID 045801, 2016.

[12] L. Wang, H. Huang, D. Shen et al., "Room temperature continuous-wave laser performance of LD pumped Er:Lu 2O3 and Er:Y2O3 ceramic at 2.7 μm," *Optics Express*, vol. 22, no. 16, pp. 19495–19503, 2014.

[13] T. Sanamyan, M. Kanskar, Y. Xiao, D. Kedlaya, and M. Dubinskii, "High power diode-pumped 2.7–μm Er3+:Y2O3 laser with nearly quantum defect-limited efficiency," *Optics Express*, vol. 19, no. 105, pp. A1082–A1087, 2011.

[14] T. Sanamyan, J. Simmons, and M. Dubinskii, "Er3+-doped Y2O3 ceramic laser at ~2.7μm with direct diode pumping of the upper laser level," *Laser Physics Letters*, vol. 7, no. 3, pp. 206–209, 2010.

[15] C. Li, J. Liu, S. Jiang et al., "2.8 μm passively Q-switched Er:CaF2 diodepumped laser," *Optical Materials Express* , vol. 6, no. 5, pp. 1570–1575, 2016.

[16] J. Liu, J. Liu, Z. Guo et al., "Dual-wavelength Q-switched Er:SrF2 laser with a black phosphorus absorber in the midinfrared region," *Optics Express*, vol. 24, no. 26, pp. 30289–30295, 2016.

[17] M. Fan, T. Li, S. Zhao et al., "Watt-level passively Q-switched Er:Lu2O3 laser at 2.84 μm using MoS2," *Optics Expresss*, vol. 41, no. 3, pp. 540–543, 2016.

[18] M. Fan, T. Li, G. Li et al., "Graphitic C3N4 as a new saturable absorber for the mid-infrared spectral range," *Optics Expresss*, vol. 42, no. 2, pp. 286–289, 2017.

[19] Z. Y. You, Y. Wang, Y. J. Sun et al., "CW and Q-switched GGG/Er:Pr:GGG/GGG composite crystal laser at 2.7 μm," *Laser Physics Letters*, vol. 14, no. 4, Article ID 045810, 2017.